Effect of Bi_2O_3 addition on the microstructure and electrical properties of the SnO_2·CoO·Nb_2O_5 varistor system

S. A. PIANARO
Departamento de Engenharia de Materiais, UEPG, 84031-510 Ponta Grossa, PR, Brazil

P. R. BUENO, P. OLIVI, E. LONGO
Departamento de Química, Universidade Federal de São Carlos, PO Box 676, 13565-905 São Carlos, SP, Brazil

J. A. VARELA
Instituto de Química, Universidade Estadual Paulista, PO Box 355, 14801-970 Araraquara, SP, Brazil

Tin dioxide (SnO_2) is an *n* type semiconductor with crystalline structure of rutile type and has low densification rate due to its high surface diffusion at low temperatures and high SnO_2 partial pressure at high temperatures [1]. Dense SnO_2 based ceramics can be achieved by introducing dopants [2–5] or by hot isostatic pressure processing [6, 7]. Dopants with valence +2 can promote densification of SnO_2 ceramics due to the formation of solid solution with the creation of oxygen vacancies.

In our previous work [8, 9] we have shown that the CoO and Nb_2O_5 doped SnO_2 ceramic is single phase and presents varistor behaviour with $Æ = 8.0$. By adding 0.05 mol% Cr_2O_3 the system is still a single phase with the non-linear coefficient increasing to $Æ = 41$.

The electrical behaviour of varistors is governed by the presence of voltage barriers at the grain boundaries [10, 11]. For a given varistor system each voltage barrier is characterized by a specific value v_b. The reference voltage barrier for a varistor is determined by the average number of barriers $\overline{n}$ in series multiplied by v_b, that is:

$$V_r = \overline{n}.v_b \quad (1)$$

Considering that $\overline{n} \propto 1/\bar{d}$, where $\bar{d}$ is the mean grain size for a given sample with width *D*, the reference voltage is given by:

$$V_r = \frac{D.V_b}{\bar{d}} \quad (2)$$

Thus, varistors for applications in low, medium and high voltage can be designed through the control of grain size and/or the sample width. Different grain size can be obtained in ZnO varistors through the use of dopants that inhibit or promote grain growth [12, 13]. However, the nature and the concentration of dopants should be controlled to avoid the degradation of the varistors' electrical properties [14, 15]. In the case of SnO_2, the CoO, Nb_2O_5 and Cr_2O_3 modulate the height and width of the voltage barriers at grain boundaries, as well as leading to different microstructures [8, 9]. The objective of this work was to verify the microstructural and electric modifications of the SnO_2·CoO·Nb_2O_5 varistor system by addition of bismuth oxide in different chemical concentrations.

The oxides used in this study were analytical grade SnO_2 (Merck), CoO (Riedel), Bi_2O_3 (Merck) and Nb_2O_5 (Aldrich). The powder compositions $(98.95 - x)$ mol% SnO_2 + 1.00 mol% CoO + 0.05 mol% Nb_2O_5 + x mol% Bi_2O_3 were obtained by conventional mixing using a ball mill. The powders were isostatically pressed in pellet shape (10.5 mm 3 1.0 mm) using a pressure of 210 MPa. The samples were then sintered in ambient air atmosphere at 1300 8C for 1 h and slowly cooled to ambient temperature. Densities were determined by geometrical measurement of the volume and by weighing the pellets in an analytical balance.

Microstructure characterizations of the sintered samples were made by scanning electron microscopy (SEM; Jeol JSM-T330A). The surface samples were polished and thermally etched at 1290 8C for 10 min to reveal the surface. Ceramic phases were determined by X-ray diffraction (XRD; Siemens D-5000).

To measure the electric properties as function of temperature a special sample holder was built and attached to the electrical oven (EDG EDGCON 3P). *I* 3 *V* electrical measurements were performed using a stabilized electrical source (Tectrol TCH 3000-2) and two digital multimeters (Fluke 8050 A). The non-linear coefficient *Æ* was obtained by linear regression of the experimental points in logarithmic scale around 1 mA cm^{-2} current and the reference electrical field was obtained in this current density. From measurements of *I* 3 *V* at several temperatures, the height of potential barrier ($_B$) and the parameters (related to the width of the potential barrier) were determined.

The electrical properties of varistors are strongly dependent on the ceramic microstructure. The microstructural variations are characterized by alterations of the average grain size and/or the presence of other ceramic phases besides the major phase. This leads to alterations of the reference voltage of the material, as predicted by Equation 2. The presence of secondary phases can be responsible for alterations of the electric properties of the material. Examples of this are the precipitation of spinel phase ($Zn_7Sb_2O_{12}$), pyrochlore ($Zn_2Bi_3Sb_3$

0261-8028

O_{14}) and different bismuth-rich phases (Æ, -, - and ^{a}-Bi_2O_3), besides others phases normally found in the ZnO varistor microstructure [16, 17]. The spinel phase consists of precipitates homogeneously distributed in the ZnO grain boundaries, and contributes to the formation of homogeneous and smaller grain size, which improves the electrical properties [18, 19]. Otherwise, the presence of ^{a}-Bi_2O_3 in the microstructure damages the electrical properties of the ceramics [19].

In earlier work [9] we showed that doping SnO_2 with 1 mol % CoO and 0.05 mol % Nb_2O_5 causes no formation of secondary phases in the microstructure, these oxides remaining in solid solution of SnO_2. The effect of the addition of different concentrations of Bi_2O_3 on the microstructure and electrical properties of the $SnO_2{\cdot}CoO{\cdot}Nb_2O_5$ system are discussed here.

Fig. 1 shows the XRD pattern of the system $(98.95 - x)$ mol % SnO_2 + 1.00 mol % CoO + 0.05 mol % Nb_2O_5 + x mol % Bi_2O_3. It was observed that there was no formation of other phases besides SnO_2. However, the ceramic presented a large variation in relative density with the addition of different amounts of Bi_2O_3, as shown in Table I. This decrease in sample density may be due to partial volatilization of added Bi_2O_3. The variation in weight loss for the system sintered at 1300 8C for 1 h as function of Bi concentration is shown in Fig. 2. Analyzing Table I, it may be observed that the sample density decreased with the addition of 0.05 mol % of Bi_2O_3 but increased with further addition of high concentrations. This indicates that the remaining concentration of Bi_2O_3 after sintering at 1300 8C is forming a solid solution with SnO_2 according to the following equation:

$$Bi_2O_3 \xrightarrow{SnO_2} 2Bi^{\bullet}_{Sn} + V^{\cdot\cdot}_{\ddot{0}} + 2O^{x}_{0} + \tfrac{1}{2}O_2(g) \qquad (3)$$

As indicated in Equation 3, the formation of solid solution in the SnO_2 lattice should increase the oxygen vacancy concentration. According to former studies, these defects facilitate the diffusion of tin through the lattice, increasing the densification of the ceramic [4].

The effect of different concentrations of Bi_2O_3 on the microstructure of SnO_2 ceramics can be seen in Fig. 3. Grain size increases with the concentration of

TABLE I Influence of Bi_2O_3 concentration on the density of the system samples $(98.95 - x)$ mol % SnO_2 + 1.00 mol % CoO + 0.05 mol % Nb_2O_5 + x mol % Bi_2O_3

Bi_2O_3 (mol %)	d_r (g cm^{-3})	Theoretical density[a] (%)
0.00	6.69	96.26
0.05	6.40	92.10
0.10	6.46	92.95
0.30	6.49	93.38
0.50	6.57	94.53

[a]Theoretical density of SnO_2, $d_T = 6.95$ g cm^{-3}

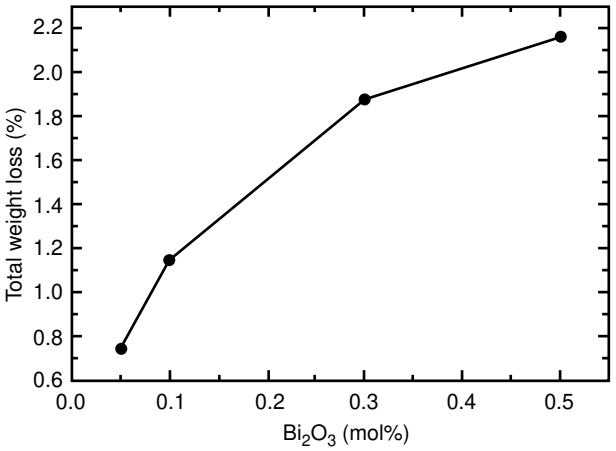

Figure 2 Weight loss as a function of Bi_2O_3 concentration in the system $(98.95 - x)$ mol % SnO_2 + 1.00 mol % CoO + 0.05 mol % Nb_2O_5 + x mol % Bi_2O_3 sintered at 1300 8C for 1 h.

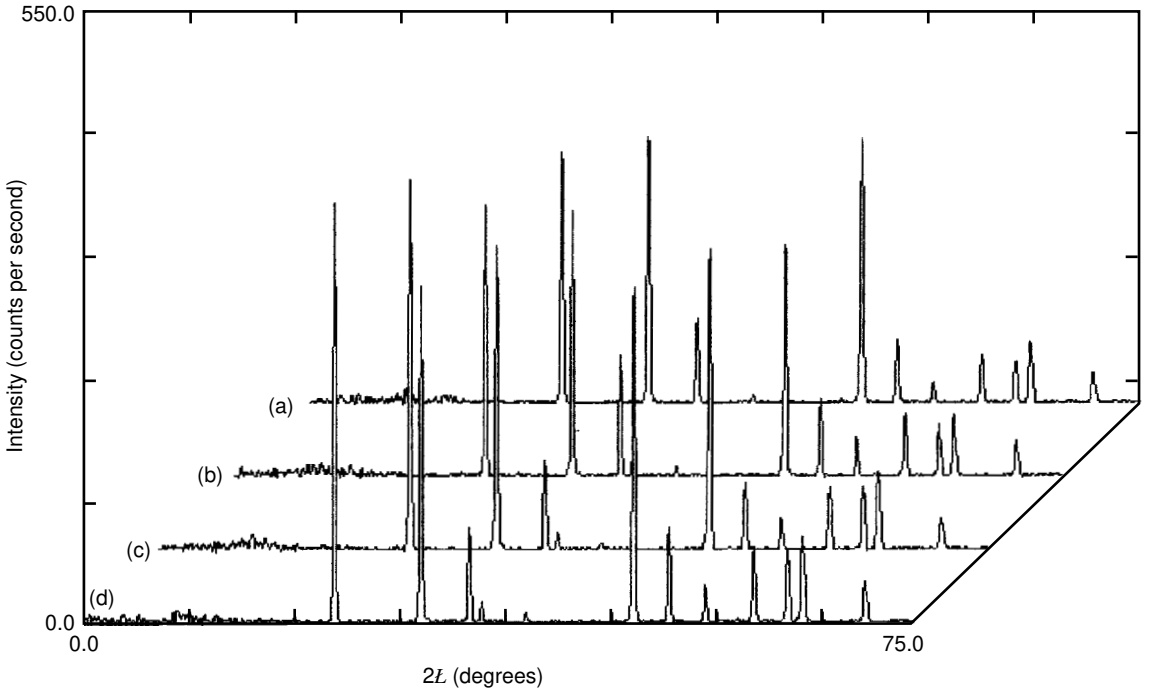

Figure 1 XRD patterns for the $(98.95 - x)$ mol % SnO_2 + 1.00 mol % CoO + 0.05 mol % Nb_2O_5 + x mol % Bi_2O_3 system. x = (a) 0.5, (b) 0.3, (c) 0.1 and (d) 0.05 mol %.

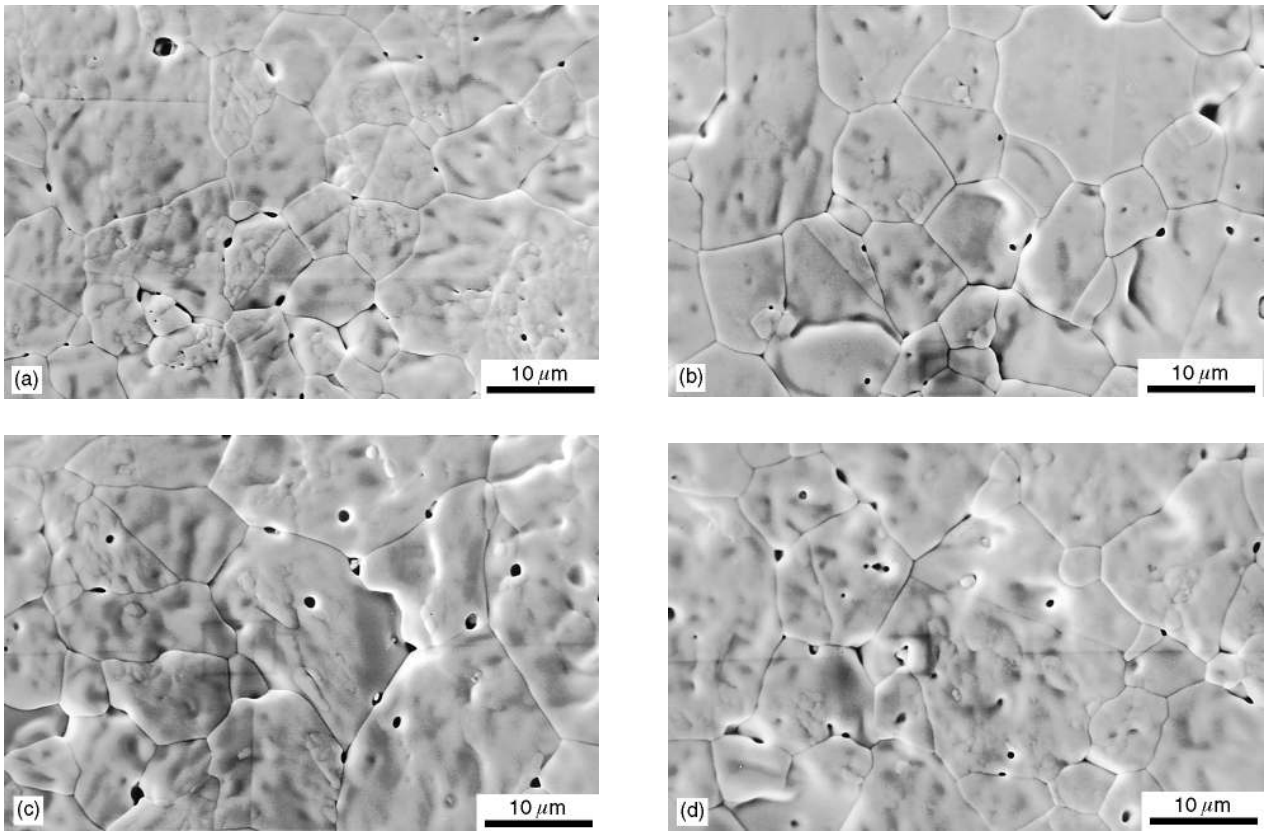

Figure 3 SEM microstructure characteristics of the $(98.95 - x)$ mol % SnO_2 + 1.00 mol % CoO + 0.05 mol % Nb_2O_5 + x mol % Bi_2O_3 system: (a) 0.05 mol % Bi_2O_3, (b) 0.1 mol % Bi_2O_3, (c) 0.3 mol % Bi_2O_3 and (d) 0.5 mol % Bi_2O_3.

Bi_2O_3. Moreover, the amount of trapped pores also increases with the concentration of Bi_2O_3. In these micrographs there is no evidence of the formation of second phase, confirming the XRD results.

The electrical characterization of these ceramics normalized in electric field E(V cm^{-1}) as a function of current density (A cm^{-2}) for different concentrations of Bi_2O_3 is shown in Fig. 4. The values of the non-linear coefficient *Æ* and the reference electric field E_r are presented in Table II. Comparing with the SnO_2 based varistor without Bi_2O_3, the non-linear characteristic of the ceramic increased with the amount of Bi_2O_3 up to 0.3 mol %. Increasing the concentration of Bi_2O_3 to 0.5 mol % caused *Æ* to decrease to its original value. However, the reference electric field decreased continuously with increasing concentration of Bi_2O_3. Considering that the reference electric field is inversely proportional to average grain size, and that grain size increase with Bi_2O_3 concentration, there is an agreement between the microstructure and the electrical measurements. The decrease in the non-linear coefficient *Æ* for 0.5 mol % Bi_2O_3 may be associated with the decrease in the average number of effective electric voltage barrier as a result of the increase in the ceramic grain size. This could also explain the increase in current leakage for this concentration of Bi_2O_3, as shown in Fig. 4.

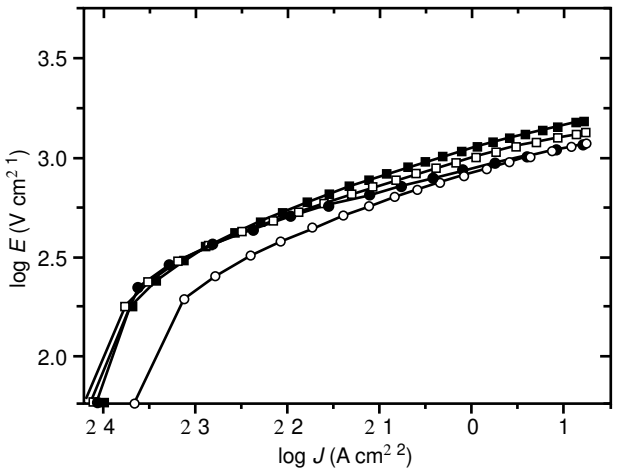

Figure 4 Influence of Bi_2O_3 concentration on the electrical behaviour of the system $(98.95 - x)$ mol % SnO_2 + 1.00 mol % CoO + 0.05 mol % Nb_2O_5 + x mol % Bi_2O_3. x = (■), 0.05; (□), 0.10; (●), 0.30; (○), 0.50 mol %.

TABLE II Effect of Bi_2O_3 concentration on *Æ* and E_r of the system $(98.95 - x)$ mol % SnO_2 + 1.00 mol % CoO + 0.05 mol % Nb_2O_5 + x mol % Bi_2O_3

Bi_2O_3 (mol %)	*Æ*	E_r (V cm^{-1})	Reference
0.00	8.00	1870	[9]
0.05	8.75	1178	This work
0.10	9.50	1061	This work
0.30	10.0	930	This work
0.50	8.00	880	This work

The addition of Bi_2O_3 to the SnO_2·CoO·Nb_2O_5 system led to ceramics with higher values of *Æ* Thus, this oxide should directly influence the grain boundary voltage barrier of this ceramic.

The effect of temperature on the E 3 J characteristic curves in the system 98.65 mol % SnO_2 + 1.00 mol % CoO + 0.05 mol % Nb_2O_5 + 0.3 mol %

Bi_2O_3 is shown in Fig. 5. The leakage current increased by two orders of magnitude when the sample temperature was raised from 28 to 166 8C. This behaviour is similar to that of the CoO and Nb_2O_5 doped SnO_2 ceramic, where the electric conduction in the ohmic region was associated with the thermion emission of Schottky type [9]. For this type of mechanism the current density is related to the electric field and temperature by the equation:

$$J_S = A^*.T^2.\exp\left[\frac{-(\ _B - \ (E^{1/2})}{kT}\right] \qquad (4)$$

where A^* is Richardson's constant, $_B$ is the interface voltage barrier height, E is the electric field and is a constant related to the potential barrier width by the relationship:

$$\propto \frac{1}{(r.\phi\ )^{1/2}} \qquad (5)$$

where r is the number of grains per unit length and ϕ is the voltage barrier width.

Considering the Schottky type conduction model, plots of $\ln J$ against $E^{1/2}$ can be built up to determine values for $_B$ and . Fig. 6 shows this type of plot for the SnO_2 based varistor doped with 0.3 mol % of Bi_2O_3 for different temperatures. The variation of the pre-exponential term of Equation 4 with temperature is very small compared with the exponential term. Thus, in the calculation of $_B$ and this term was neglected.

The current density is strongly dependent on temperature for low electric field. However, for higher values of E this dependence decreases, approaching complete temperature independence. The curves of Fig. 6a, for different temperatures, were extrapolated to $E = 0$, as shown in Fig. 6b, then values of $\ln J$ for $E = 0$ were plotted against $1/T$, as shown in Fig. 7. Values of and $_B$ were determined from the plots of Figs 6 and 7, and are shown in Table III.

The results of Table III show that Bi_2O_3 helps the formation of higher and narrower grain boundary voltage barrier as compacted with the SnO_2 system without this dopant. This leads to a higher non-linear characteristic of this ceramic. Contrary to the ZnO

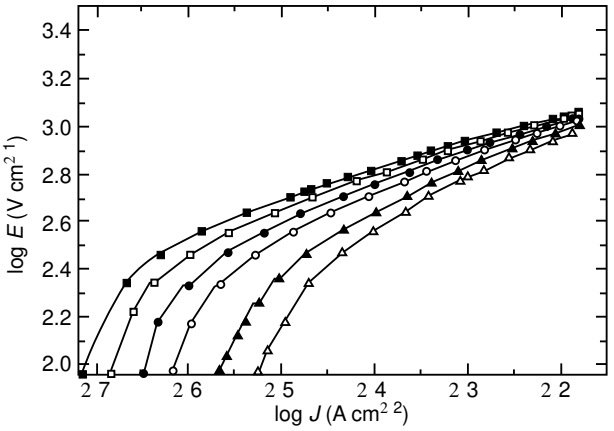

Figure 5 Influence of temperature on the electrical conduction characteristic of the system 98.65 mol % SnO_2 + 1.00 mol % CoO + 0.05 mol % Nb_2O_5 + 0.3 mol % Bi_2O_3. (■), 28; (□), 55; (●), 82; (○), 109; (▲), 137; (△), 166 8C.

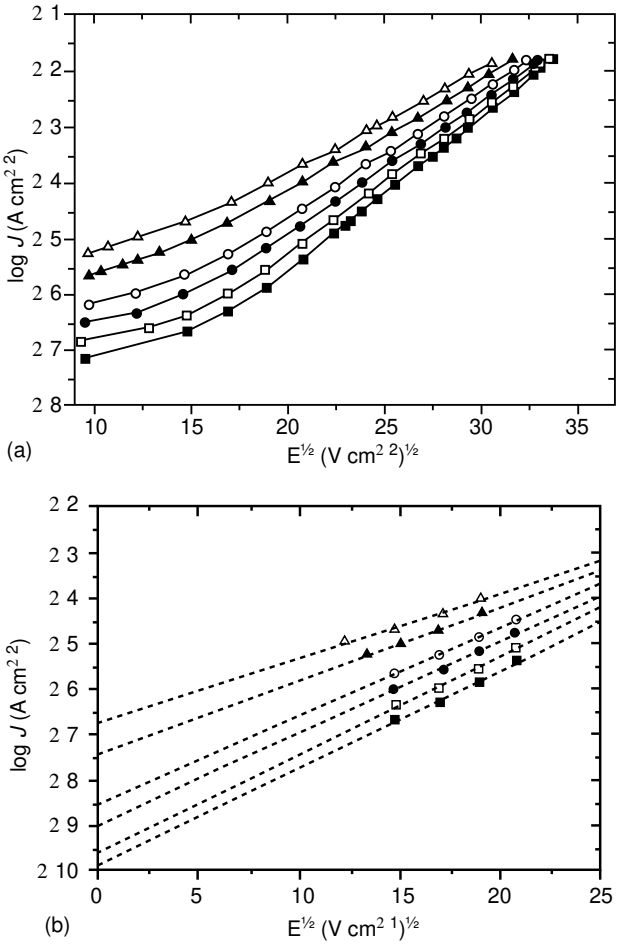

Figure 6 (a) Characteristic plots of $\ln J$ 3 $E^{1/2}$ for the 98.65 mol % SnO_2 + 1.00 mol % CoO + 0.05 mol % Nb_2O_5 + 0.3 mol % Bi_2O_3 system. (b) Extrapolation of the straight lines of plot (a) to $E = 0$. (■), 28; (□), 55; (●), 82; (○), 109; (▲), 137; (△), 166 8C.

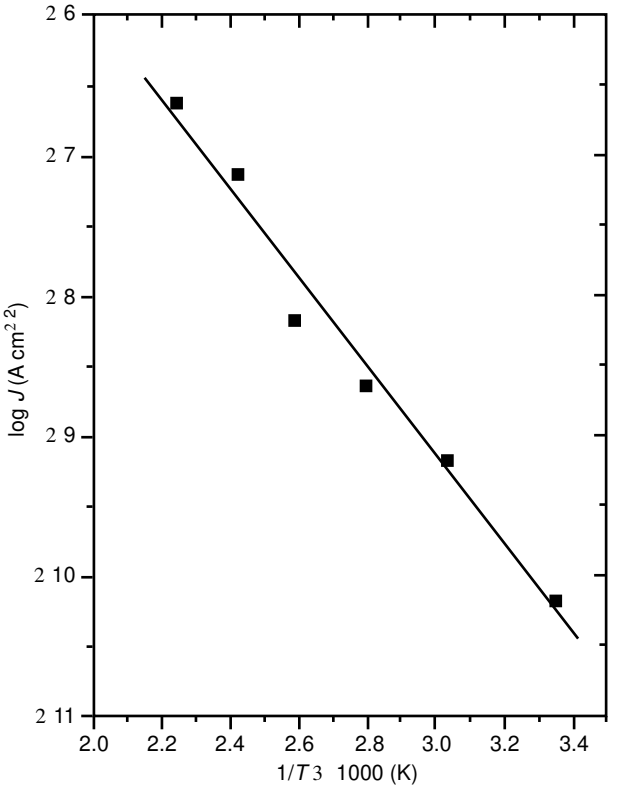

Figure 7 Characteristic plot of $\ln J$ 3 $1/T$ for $E = 0$ of the 98.95 mol % SnO_2 + 1.00 mol % CoO + 0.05 mol % Nb_2O_5 + 0.3 mol % Bi_2O_3 system.

TABLE III Calculated values for voltage barrier height ($_B$) and width (ϕ)

System	$_B$	3 10^3 ($V^{-1/2}$ $cm^{1/2}$)	References
SnO_2·CoO·Nb_2O_5	0.49	7.10	[9]
SnO_2·CoO·Nb_2O_5·Bi_2O_3	0.63	12.3	This work

based varistor, secondary phase was apparently not observed in this Bi_2O_3 doped SnO_2 system. In this system it is believed that the voltage barrier is formed due to the creation of atomic defects at ceramic grain boundaries. According to Equation 3, the Bi_2O_3 should contribute to the increase of negative charges due to the creation of the atomic defect $Bi_{Sn}^{\bullet}$ at the interface, inducing the formation of positive oxygen vacancies. These positive defects are located at the depletion layer of width ϕ. Then, according to the former proposed model [9], the bismuth oxide should be responsible for the increase in defect concentration at the ceramic grain boundaries improving the electric properties of the SnO_2 based varistor.

Several studies about the importance of Bi_2O_3 on the conduction mechanism of ZnO have been conducted in the literature. Firstly, it was believed that the presence of voltage barrier at the grain boundaries would result in the formation of a continuous bismuth-rich phase of high resistivity between the grains [14]. However, further studies demonstrated that the majority of grains are not separated by this continuous bismuth-rich phase, but are located at the multiple grain junctions [20, 21]. However, some studies showed the existence of a Bi_2O_3 thin film tens of nanometres wide separating the ZnO grains [22, 23].

In the case of the Bi_2O_3 doped SnO_2 ceramics studied in this work, there was no formation of a continuous bismuth-rich phase between the grains or precipitation of Bi_2O_3 phase at the multiple grain junctions. Up to now no bismuth-rich thin film has been observed between the SnO_2 grains. If this film exists it has no large influence on the electrical properties of the material. Although the non-linearity of the SnO_2 based ceramic increased with the addition of Bi_2O_3, this increase was very small compared with the SnO_2·CoO·Nb_2O_5 system. This increase in non-linearity should be credited to the atomic defects created by Bi_2O_3 due to its substitution in the SnO_2 lattice, according to Equation 3.

In conclusion, the addition of up to 0.3 mol% bismuth oxide in the SnO_2·CoO·Nb_2O_5 system increased the non-linear coefficient of the ceramic. Larger grains are formed with addition of this oxide and ceramics with lower reference electric fields are obtained. The increase of the non-linear coefficient with addition of Bi_2O_3 is probably due to the increase of atomic defect concentration at the SnO_2 grain boundaries, which contributes to the formation of Schottky type voltage barrier. Thus, higher and narrower voltage barriers are formed with the addition of Bi_2O_3 to the basic SnO_2·CoO·Nb_2O_5 system.

Acknowledgements

The authors acknowledge FINEP/PADCT, CNPq and FAPESP, all Brazilian agencies, for the financial support of this work.

References

1. Z. M. JARZEBSKI and J. P. MARTON, *J. Electrochem. Soc.* **123** (1976) 299C.
2. J. A. VARELA, *Cerâmica* **31** (1985) 241.
3. J. F. MCALER, P. T. MOSELEY, J. O. W. NORRIS and D. E. WILLIAMS, *J. Chem. Soc. Faraday Trans.* **83** (1987) 1323.
4. J. A. VARELA, O. J. WHITTEMORE and E. LONGO, *Ceram. Int.* **16** (1990) 177.
5. J. A. CERRI, E. R. LEITE, D. GOUVÊA, E. LONGO and J. A. VARELA, *J. Amer. Ceram. Soc.* **79** (1996) 799.
6. T. KIMURA, S. INADA and T. YAMAGUCH, *J. Mater. Sci.* **24** (1989) 220.
7. M. K. PARIA and H. S. MAITI, *ibid.* **18** (1983) 2101.
8. S. A. PIANARO, P. R. BUENO, E. LONGO and J. A. VARELA, *J. Mater. Sci. Lett.* **14** (1995) 692.
9. S. A. PIANARO, P. R. BUENO, P. OLIVI, E. LONGO and J. A. VARELA, *J. Mater. Sci.* submitted.
10. W. G. MORRIS, *J. Vacuum Sci. Technol.* **13** (1976) 926.
11. J. WONG, *J. Appl. Phys.* **47** (1976) 4971.
12. J. MATSUOKA, *Jpn. J. Appl. Phys.* **10** (1971) 736.
13. K. EDA, M. INADA and M. MATSUOKA, *J. Appl. Phys.* **54** (1983) 1095.
14. T. K. GUPTA, *J. Amer. Ceram. Soc.* **73** (1990) 1817.
15. S. A. PIANARO, E. C. PEREIRA, L. O. S. BULHÕES, E. LONGO and J. A. VARELA, *J. Mater. Sci.* **30** (1995) 133.
16. M. INADA, *Jpn. J. Appl. Phys.* **17** (1978) 1.
17. *Idem, ibid.* **17** (1978) 673.
18. S. PIANARO, Ms thesis, University Federal of Sao Carlos, Brazil (1990).
19. T. TAKEMURA, M. KOBAYASHI, Y. TAKADA and K. SATO, *J. Amer. Ceram. Soc.* **70** (1987) 237.
20. D. R. CLARKE, *J. Appl. Phys.* **49** (1978) 2407.
21. H. KANAI, M. IMAI and T. TAKAHASHI, *J. Mater. Sci.* **20** (1985) 3957.
22. L. M. LEVINSON and H. R. PHUILIPP, *J. Appl. Phys.* **46** (1975) 1332.
23. J. WONG, *J. Am. Ceram. Soc.* **57** (1974) 357.

Received 2 July
and accepted 13 November 1996